JOURNAL OF THERMOPHYSICS AND HEAT TRANSFER
Vol. 20, No. 3, July–September 2006

# Shock-Tube Measurement of Nitridation Coefficient of Solid Carbon

Chul Park* and David W. Bogdanoff†
*Eloret Corporation, Sunnyvale, California 94087*

**The coefficient of reaction of nitrogen atoms with solid carbon to form gaseous cyanogen CN is measured in a shock tube. A stream of highly dissociated nitrogen is produced in a shock tube and passed over a grid of metal wire coated with carbon. The radiation emitted by the wake of the wire grid is observed with a monochromator set at 386 nm, where CN is known to radiate strongly. From the intensity of the CN radiation, the concentration of CN in the wake is determined. The concentration of nitrogen atoms in the stream are calculated by integrating conservation equations. From these concentration values, the fraction of the collisions of nitrogen atoms producing CN, that is, the reaction coefficient, is deduced. The results show that the reaction coefficient is about 0.3 at both 300 and 1100 K. The uncertainties in the results are described, and improvements are proposed.**

## Introduction

IN the future, spacecraft may be returning from planetary, asteroidal, or cometary missions and entering Earth's atmosphere at a superescape velocity. The shock layer formed during the entry flight around such a vehicle will be nearly totally dissociated and partially ionized. Carbonaceous materials are favored as the heatshield material for such vehicles because they can absorb high heating rates occurring in such entries. (See, for example, Refs. 1 and 2.)

Such carbonaceous heatshields are made by impregnating a graphitic matrix with a hydrocarbon resin and curing at an elevated temperature. During the entry flight, the resin pyrolyzes, and the resulting gas diffuses through the material and escapes from the surface. The ablating surface becomes nearly pure carbon. The pyrolysis process produces condensation of solid carbon. Most of the solid carbon becomes trapped inside the graphitic matrix in a process known as coking. However, some of the carbon formed could escape from the material in the form of small particles, as shown schematically in Fig. 1. References 3 and 4 present evidence for the presence of such small carbon particles in the shock-layer flow. These solid particles can affect the heat transfer process in several different ways. (See, for example, Ref. 4.)

Studies to date indicate that boundary-layer flows over the ablating surface in such entry flights are in a chemical nonequilibrium state. (See, for example, Ref. 1.) The three-body recombination processes

$$O + O + M \rightarrow O_2 + M$$

$$N + N + M \rightarrow N_2 + M$$

are too slow to remove the atomic species in the relatively cold boundary layer. As a result, oxygen and nitrogen atoms present at the edge of the boundary layer can survive through the diffusion process to reach the carbon surface. It is well known that the atomic oxygen reacts with solid carbon to form carbon monoxide (CO) through the oxidation process

$$O + C(c) \rightarrow CO + 3.74\ \text{eV} \tag{1}$$

wherein ($c$) signifies a crystalline, that is, solid, state. The reaction coefficient of this process, that is, the fraction of said collisions of O atoms producing CO, has been measured in atomic beam experiments. (See the references cited in Ref. 5.) In such experiments, a beam of atomic oxygen was made to hit a solid carbon surface at an energy of a few electron volts equivalent to a few tens of thousands of degrees. Such experiments have shown that the reaction coefficient is independent of the energy of the colliding O atoms and is a function only of the temperature of the solid. The coefficient was found to vary from about 0.01 at room temperature to about 0.3 at 3000 K wall temperature.[5]

The consequence of process (1) is to increase the rates of ablation and the heating. Question arises as to whether atomic nitrogen will undergo a similar process, that is, whether the nitridation process

$$N + C(c) \rightarrow CN + 0.35\ \text{eV} \tag{2}$$

can occur. If this reaction occurs, the CN molecules so produced are likely to undergo the exchange reaction in the gas phase

$$N + CN \rightarrow N_2 + C + 2.04\ \text{eV} \tag{3}$$

Because the reaction is exothermic and, consequently, fast, it will tend to reach equilibrium in most of density regime of practical interest. As a result, $N_2$ and C are formed, and the net heat generated by the nitridation process is nearly equal to that of the oxidation process, Eq. (1). Heat transfer rate will increase significantly as a result.[6]

The coefficient for the nitridation reaction, Eq. (2), is presently unknown. It is the purpose of the present work to determine this reaction coefficient experimentally.

The atomic beam method used successfully in the past for studying the oxidation process involves two essential steps: 1) producing a beam of atomic oxygen of known flux value and 2) reliably measuring the flux of the product of the surface reaction, CO. Both of these steps rely, in turn, on being able to calibrate the sensitivity of the flux-measuring device.

The beam method is not suitable for the nitridation process because 1) producing a beam of nitrogen atoms to a known flux is difficult, and 2) calibrating the mass spectrometer for CN is also difficult because CN is thermochemically unstable.

Another existing method for measuring a surface reaction rate is one in which the rate of removal of gas species at the reacting surface is deduced from the rate of diffusion from the source of the

Presented as Paper 2003-0158 at the 41st Aerospace Sciences Meeting, Reno, NV, 6–9 January 2003; received 26 September 2005; revision received 15 November 2005; accepted for publication 19 November 2005. 

*Senior Research Scientist; currently Professor, Department of Aerospace Engineering, Korea Advanced Institute of Science and Technology, 373-1 Guseong-dong, Yuseong-gu, Daejeon, 305-701, Republic of Korea; cpark216@kaist.ac.kr. Fellow AIAA.

†Senior Research Scientist, Mail Stop 230-1, NASA Ames Research Center, Moffet Field, CA 94035; bogdanoff@mail.arc.nasa.gov. Associate Fellow AIAA.

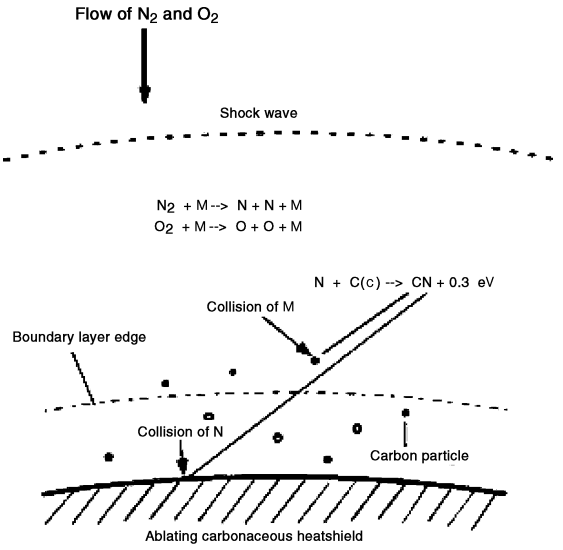


**Fig. 1 Schematic of shock-layer flow showing occurrence of nitridation phenomenon.**

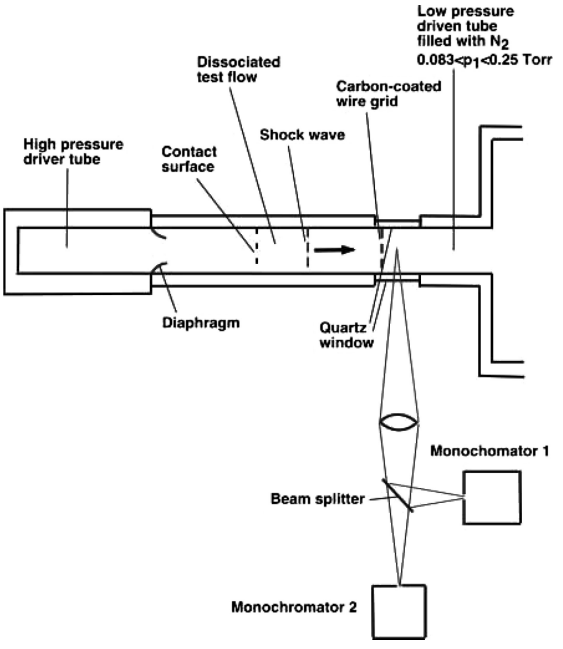


**Fig. 2 Schematic of experimental setup in Electric Arc Shock-Tube facility at NASA Ames Research Center.**

reacting species to the reacting surface.[7] This scheme is appropriate when the rate of removal of the species by the surface reaction is of the same order as the diffusion rate and is suitable for relatively slow surface reactions. Unfortunately, as seen from the example of the oxidation process (and as the results of the present work will show), the surface nitridation rate is too fast for the diffusion rate to respond. Therefore, this scheme is also considered unsuitable.

A new method is devised in the present work. In this method, low-density nitrogen atoms are flowed past a screen or grid of carbon wires. Such a flow is easily produced in a shock tube. The collisions of the nitrogen atoms with the carbon wires produces CN. The concentration of CN in the wake of the grid is determined spectrometrically. When the rate of production of CN thus determined is divided by the rate of collisions of atomic nitrogen against the carbon wires, the reaction coefficient is determined.

## Method

The shock-tube experiment is conducted in the Electric Arc Shock-Tube facility of NASA Ames Research Center.[8,9] The experimental setup is shown schematically in Fig. 2. The internal diameter

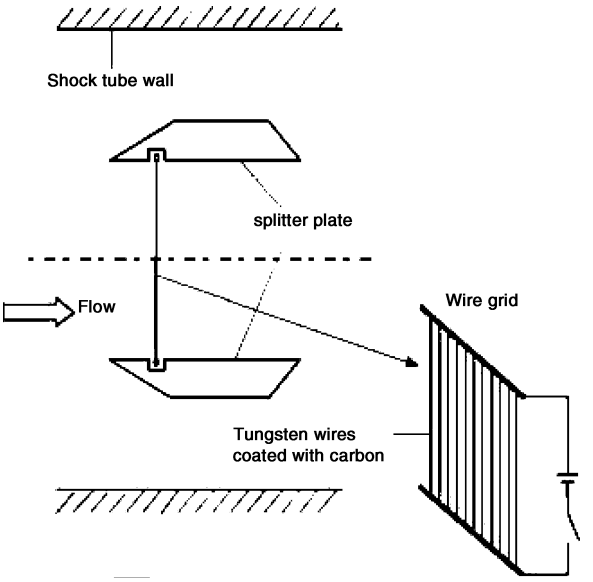


**Fig. 3 Schematic side view of splitter and wire grid arrangement in test section.**

is 10 cm for both the driver and driven sections. Both sections are made of stainless steel. The driver is conical in shape (Fig. 2 showing a cylindrical driver only for schematic purposes) and is 23.5 cm in length.[8] The diaphragm, made of aluminum, ruptures because of the pressure rise resulting from arc discharge. The test section is 5.34 m downstream of the diaphragm.

The driver is filled with helium to a pressure of about 6.8 atm. The driven section is filled with high-purity nitrogen to a pressure $p_1$ of either 0.083 or 0.25 torr. An electrical current is passed through the driver gas by exploding a tungsten wire. The speed of the primary shock wave produced varied between 8200 and 8700 m/s. The calculated pressure behind the primary shock wave varied between 0.08 and 0.4 atm. The calculated frozen-flow Rankine–Hugoniot temperature for the heavy particles is about 33,000 K; the equilibrium degree of dissociation achieved is about 0.8; and the equilibrium temperature is about 7000 K in the flow behind the primary shock wave.

The grid of tungsten wire coated with carbon is placed in the test section as shown schematically in Fig. 2. The grid consists of 22 tungsten wires 0.0508 mm in diameter, spaced at 2.39-mm intervals and coated with carbon, as indicated schematically in Fig. 3. The splitter plates placed at the top and the bottom of the grid are for the purpose of minimizing the influence of boundry-layer growth on the shock-tube wall onto the wire grid. The wires are heated by passing an electrical current through them. The power source is an automobile battery, and the wires are heated to the desired temperature roughly 3 s before the shock tube is fired. A current of about 6.7 A total at a voltage of about 1.6 V is passed through the grid to heat the wires to about 1050 K. The temperature of the wires is determined from the well-known temperature-to-resistance relathionship characteristics of tungsten wires.

Before it is mounted inside the shock tube, the tungsten wire grid is coated with carbon through the well-known graphitization process. The wire grid is first passed 10 times through the combined flame of a row of candles, causing a layer of lampblack to form on the wire surface. The grid is then heated electrically in vacuum for about 5 s to a temperature of about 1100 K to drive off the volatile component of the lampblack and to carbonize. The emissivity of the resulting wire surface, determined from the electrical power required to attain a set elevated temperature, was very nearly unity. This heating process assured that the lampblack is converted mostly to graphitic carbon.

Visual inspection of the wires after a test showed that the graphitic carbon layer remained intact throughout a test. There was no visible change in the surface structure. This means that the interaction between the flow and the wire surface occurs in the molecular scale.

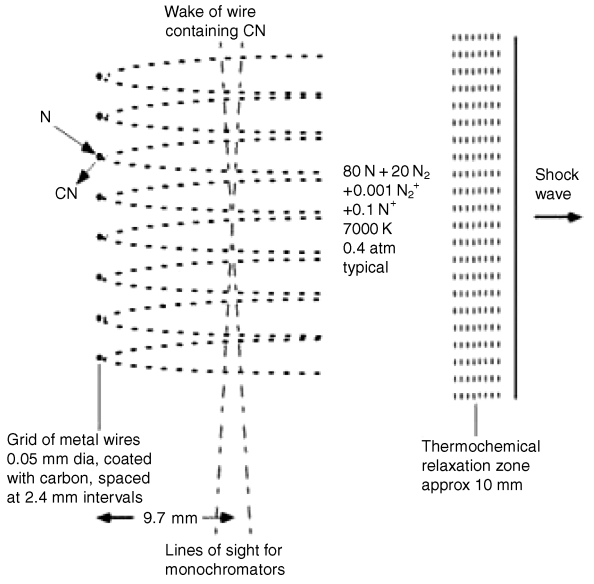


**Fig. 4 Schematic of top view of wake region of wire grid.**

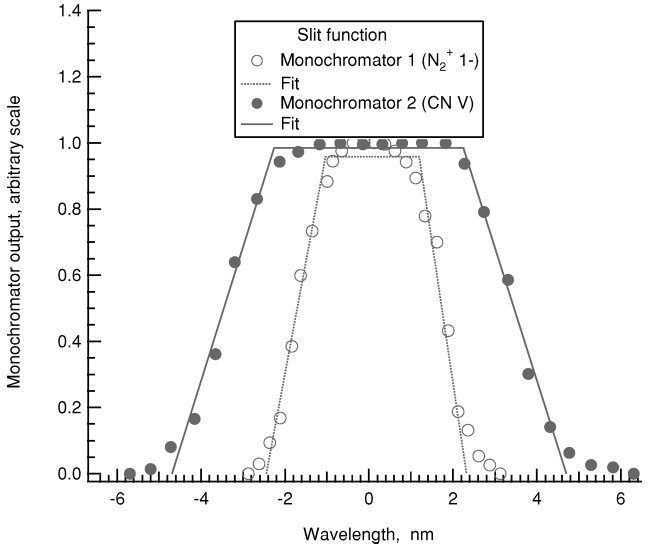


**Fig. 5 Slit function for monochromators.**

A spectral intensity measurement is made across the flow through the lines of sight located about 9.7 mm downstream of the wire grid, as shown schematically in Fig. 4. The radiation power collected by a lens is split into two monochromators, 1 and 2, using a beam splitter as shown schematically in Fig. 2. As the dissociated test flow passes through the grid, nitrogen atoms strike the wires. If the surface reaction process (2) occurs, there will be CN molecules in the wake of the wires as shown schematically in Fig. 4.

The two monochromators are made by Bausch and Lomb and have a focal length of 25 cm. The slit function for the two monochromators is shown in Fig. 5. A trapezoid is fitted to represent the observed slit function, as shown. The center of the slit function of monochromator 1 is set at 391.2 nm to collect the radiation emanating mostly from the (0–0) band of the $N_2^+$ first negative (1−) system. The center of monochromator 2 is set at 386.3 nm to collect the radiation emanating from the (0–0), (1–1), (2–2), (3–3), etc., bands of the CN violet system. The depth of view of the test gas is 52.4 mm. The sensitivity of the monochromators is calibrated absolutely using a standard tungsten ribbon lamp. The lamp is placed at the center of the test section to produce the same optical arrangement as in measurement. From the output from monochromator 2, the concentration of CN is determined using the latest version of the nonequilibrium air radiation (NEQAIR) code,[10] assuming Boltzmann distribution of internal states.

The concentration of nitrogen atoms striking the carbonized wires is calculated theoretically, accounting for thermochemical nonequilibrium using the one-dimensional continuum flow code developed in Ref. 11. The accuracy of the calculation procedure has been verified previously by comparison with a spectroscopic experiment in Ref. 12. The number of collisions between the nitrogen atoms and the wires is determined assuming a free-molecular flow. The Knudsen number based on the wire diameter for nitrogen atoms is about one for the $p_1 = 0.25$ torr case and about three for the 0.083-torr case, which allows, within a small error, the free-molecular assumption. The fractional frontal area of the wires is as follows: The fractional frontal area equals the wire diameter/wire spacing = 0.0508/2.39 = 0.0213.

By the definition of the reaction coefficient, the number of CN molecules formed within a 1-cm width within 1 s equals the number of N atoms passing within a 1-cm width within 1 s times the fractional frontal area times the reaction coefficient. Therefore,

$$\text{Reaction probability} = \frac{\text{CN concentration}}{\text{N concentration}} \div 0.0213 \qquad (4)$$

The uncertainty in the calculated concentration of atomic nitrogen due to the uncertainty in the rate coefficicient for the dissociation of $N_2$ is insignificant, as will be shown later.

The main uncertainty in this method of determining the reaction probability is the effect of the CN-removal reaction, Eq. (3). Reference 13 gives the rate coefficient of the reaction CN + N → C + $N_2$ as $6.3 \times 10^{13}$ cm$^3$/(mol · s). Using this reaction rate value, one finds that approximately 30% of the CN is removed by reaction (3) within the 9.7-mm distance between the wire grid and the optical measuring position for $p_1 = 0.25$ torr. For $p_1 = 0.083$ torr, approximately 10% of the CN is removed. The impact of this phenomenon on the value of the reaction probability deduced will be discussed later.

## Results

### Without Carbon Coating on Wire

The successful runs are summarized in Table 1. In Table 1, the measured driven tube charging pressure $p_1$, shock velocity $U_s$, and wire temperature $T_w$ are believed to be accurate to within 1, 3, and 2%, respectively. A typical result of the theoretical flowfield calculation is shown in Fig. 6. According to Fig. 6, equilibrium is not reached within 8 cm behind the shock wave. The mole fraction of nitrogen atoms is already high at 1 cm behind the shock wave and remains relatively constant thereafter, indicating a quasi steady state there.

The outputs from the two monochromators are shown in Figs. 7a and 7b for run 11, which was made without the carbon coating on the wire. (Note that the porarity of the output signal is negative.) Figures 7a and 7b suggest that the useful test time is at least 5 $\mu$s, which corresponds to about 4 cm for the present shock velocity range from 8200 to 8700 m/s. From this, the useful test time is assumed to be 5 $\mu$s in the remainder of the present work. The nonequilibrium radiation overshoot phenomenon expected[12] in such a nonequilibrium

**Table 1 Successful runs**

| Run no. | $p_1$,[a] torr | $U_s$,[b] m/s | N carbon | | $T_w$,[c] K | Reaction coefficient |
|---|---|---|---|---|---|---|
| | | | Fraction | Coating | | |
| 6 | 0.25 | 8381 | 0.808 | Yes | 970 | 0.190 |
| 7 | 0.25 | 8287 | 0.793 | Yes | 1056 | 0.230 |
| 8 | 0.25 | 8408 | 0.813 | Yes | 300 | 0.155 |
| 9 | 0.25 | 8403 | 0.813 | No | NA | NA |
| 10 | 0.25 | 8358 | 0.805 | Yes | 300 | 0.160 |
| 11 | 0.25 | 8358 | 0.808 | No | NA | NA |
| 12 | 0.25 | 8512 | 0.829 | Yes | 1040 | 0.218 |
| 13 | 0.25 | 8759 | 0.865 | Yes | 1060 | 0.161 |
| 16 | 0.083 | 8432 | 0.742 | Yes | 1106 | 0.303 |
| 18 | 0.083 | 8409 | 0.739 | Yes | 300 | 0.272 |

[a]Driven tube charging pressure. [b]Shock velocity. [c]Wire temperature.

flow is seen prominently in Figs. 7a and 7b as a (negative) voltage spike at about 472 $\mu$s.

The theoretical output from the two monochromators is calculated using the results of the flow calculation such as that shown in Fig. 6. The calculation indicates that the first negative band of $N_2^+$, which emanates from the B state located at 25461 $cm^{-1}$ above the ground state, is in a Boltzmann distribution relative to the ground electronic state after about 0.5 $\mu$s. Therefore, the Boltzmann assumption is made for the first negative band. In the wavelength range covered by monochromator 1, the second positive system of $N_2$ radiates. This system emanates from the $C^3\Pi_u$ state lying at 89,137 $cm^{-1}$ above the ground state of $N_2$, substantially higher than the dissociation limit of 78,740 $cm^{-1}$ for $N_2$. Therefore, under the prevailing nonequilibrium environment, the population of the state is difficult to determine. The NEQAIR code does not calculate the population of this state. Therefore, the amount of radiation is bounded by assuming that this state is in Boltzmann equilibrium with the ground electronic state or is zero.

The calculated output values for monochromator 1 are compared with the experimental data in Fig. 7a. As Fig. 7a shows, the experimental data from monochromator 1 fall between the two calculated limits. The observed nonequilibrium overshoot is bounded by the two sets of theoretical values. The experimental data after about 1.5 $\mu$s agree approximately with the calculation, indicated in Fig. 7a as the adjusted prediction. This adjusted prediction assumes that the number density of the upper state of the second positive system is 20% of the equilibrium value. This distribution was selected to best fit the experimental data. As will be shown later, this uncertainty in the intensity of the $N_2$ second positive system does not affect the final results. The procedure is exercised only to confirm that the observed phenomena are compatible with the current understanding of the problem.

The theoretically predicted output from monochromator 2 obtained using this adjusted strength of the second positive system is shown in Fig. 7b. As seen, the measured output is considerably stronger than the value calculated accounting only for $N_2^+$ first negative and $N_2$ second positive systems. The measured data can be numerically reproduced by assuming that the flow contained CN to a concentration of 0.006%, that is, 60 ppm. Calculation shows that this amount of CN does not affect the output from monochromator 1.

This trace amount of CN in the flow may be attributable to the plastic electric insulator components present in the test section or to other contamination sources. In any case, the CN concentration of this amount has little effect on the present test because the concentration of CN produced by the intended surface reaction is at least an order of magnitude larger, as will be shown later.

The theoretical spectrum for the assumed gas mixture is shown in Fig. 8. Figure 8 shows also the locations and the slit functions of the two monochromators in the wave-length space. As seen here, the two monochromators capture well the respective intended radiation,

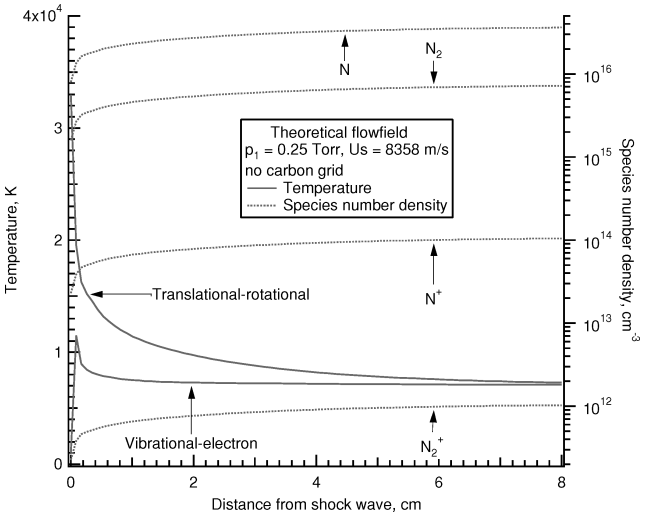


**Fig. 6 Calculated distribution of properties behind shock wave.**

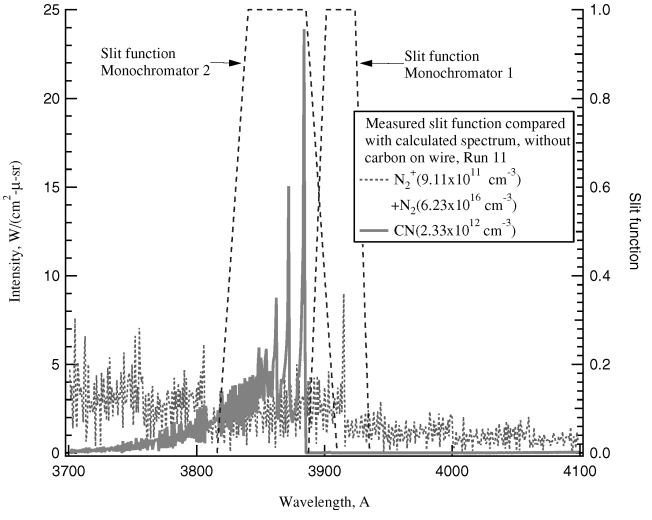


**Fig. 8 Calculated spectrum for no-carbon case, run 11, and slit functions.**

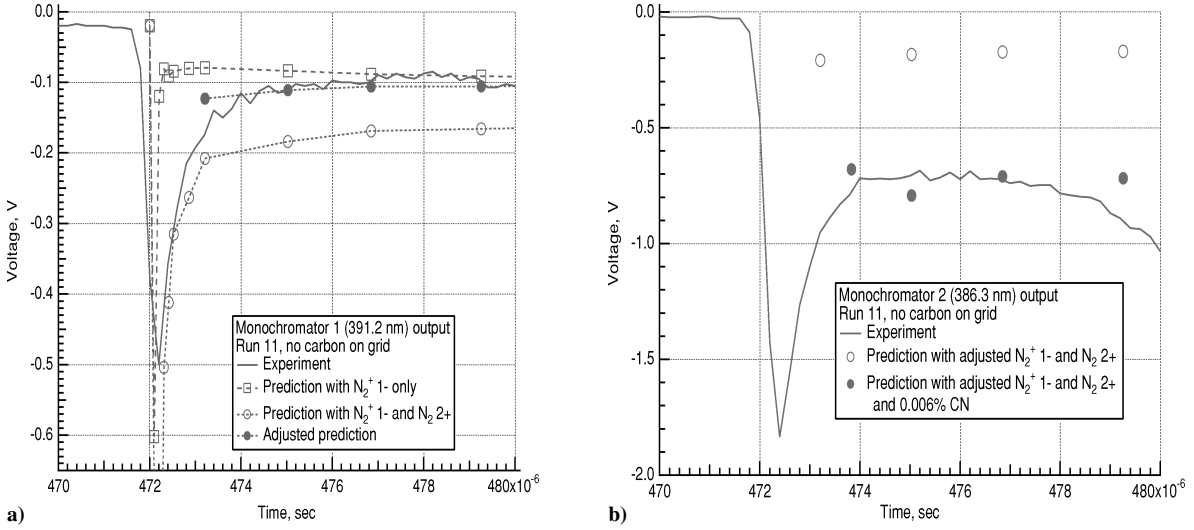


**Fig. 7 Output from monochromators for run 11, without carbon coating on wire: a) monochromator 1, centered at 391.2 nm and b) monochromator 2, centered at 386.3 nm.**

that is, the $N_2^+$ first negative for monochromator 1 and CN violet for monochromator 2.

Typical voltage outputs from the two monochromators with carbon-coated wires are shown in Fig. 9 for the case of $p_1 = 0.25$ torr. The case of $p_1 = 0.083$ torr is shown in Fig. 10. As indicated in Figs. 9 and 10, monochromator 2 was masked with a neutral density filter of optical density 1.1 (a factor of $10^{1.1} = 12.6$) for the 0.25-torr case and 0.9 (a factor of $10^{0.9} = 7.94$) for the 0.083-torr case, to prevent the signals from moving out of scale. For both cases, the output levels for monochoromator 2, after the passage of the nonequilibrium peak, are much higher than that seen in Fig. 7b. Thus, the nonequilibrium overshoot phenomenon appears insignificant.

For the $p_1 = 0.25$ torr case, Fig. 9, the magnitude of the voltage output increases with time beyond the minimum reached at around 469.5 $\mu$s. This feature was seen in all $p_1 = 0.25$ torr runs. The exact reason for this increase is unknown. However, suspicion exists that the carbon coating is outgassing hydrocarbon compounds when heated suddenly by the flow, as would happen if the graphitization of the carbon coating is imperfect. More thorough graphitization, possibly by a method other than the lampblack technique used in the present work, could eliminate such possibilities. This point will be considered in the "Future Work" section. For the $p_1 = 0.083$ torr

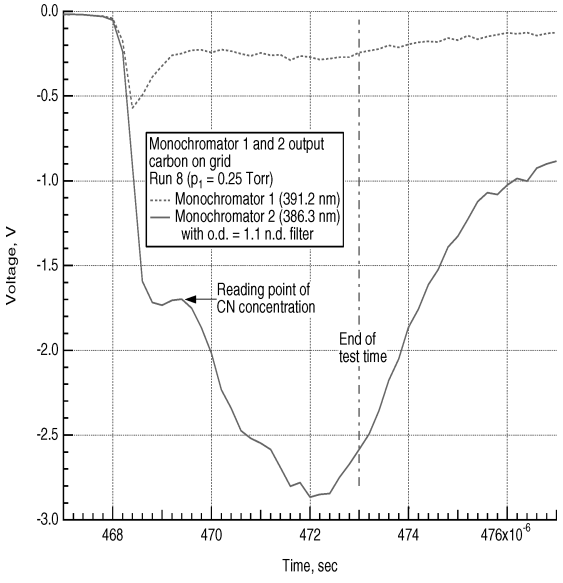


**Fig. 9 Outputs from monochromators for run 12, $p_1 = 0.25$ torr.**

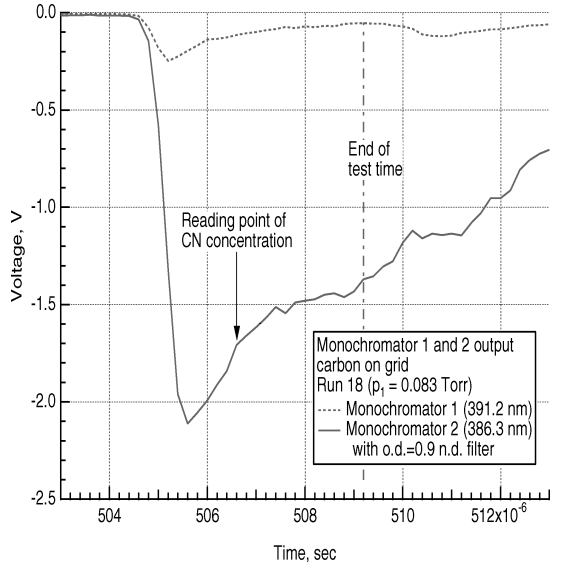


**Fig. 10 Outputs from monochromators for run 18, $p_1 = 0.083$ torr.**

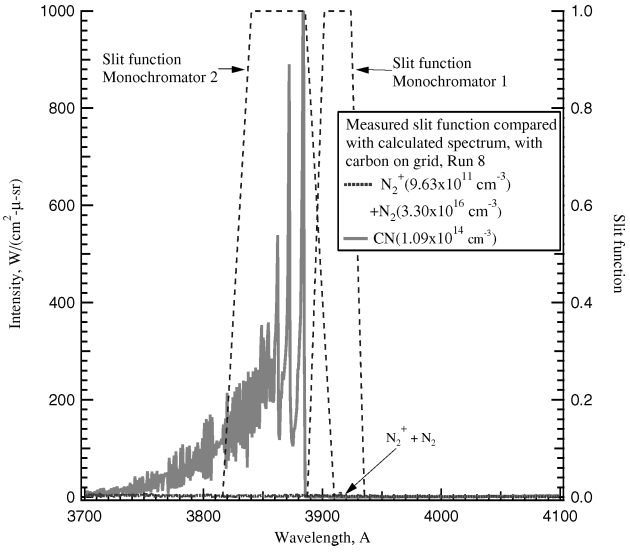


**Fig. 11 Calculated spectrum for carbon-coated case, run 8, and slit function.**

case, Fig. 10, this increase in output level does not occur, possibly because the heating by the flow is weak. For the $p_1 = 0.25$ torr cases, the output value at the lowest point was used to determine CN concentration.

The monochromator 2 output was used to determine the number density of CN by matching the calculated output with the measured value. From the CN concentration determined in that way and from the calculated concentration of nitrogen atoms, the reaction probability is determined using Eq. (4). The results are presented in Table 1.

In Fig. 11, the spectrum calculated for the carbon-coated case, is shown. Note that the scale of the ordinates is 40 times that of the no-carbon case, Fig. 8. The radiation by $N_2^+$ first negative and $N_2$ second positive systems in the 391-nm region is negligibly weak compared with the radiation in the 386-nm region. This result assures that the uncertainty about the contribution of the $N_2$ second positive system to the monochromator 1 output is inconsequential.

Another uncertainty in the calculated reaction probability values concerns the rate coefficient for the dissociation of $N_2$. A slower dissociation rate has an effect of scaling up the abscissa in Fig. 6, causing the calculated N-atom concentrations to be smaller at a fixed disance. If the true dissociation rate were a factor of three slower than that assumed in the calculation, the N-concentration value will be about 20% smaller in the region of interest. According to Eq. (6), this leads to a 20% larger reaction probability value. However, as Table 1 shows, the spread in the determined reaction probability value is larger than 20%. On the other hand, a faster dissociation rate decreases the reaction probability value, but to a smaller extent.

In Fig. 12, the reaction probability values determined in the present work are shown in an Arrhenius plot. As mentioned in the "Method" section, these probability values tend to underestimate because the CN-removal reaction (3) is not accounted for. As mentioned, for the case of $p_1 = 0.25$ torr, the reaction removes about 30% of the CN molecules between the wire and the optical measuring position. For $p_1 = 0.083$ torr, about 10% is removed. Figure 12 shows that the $p_1 = 0.25$ torr data are lower than the $p_1 = 0.083$ torr data by about 10–30%, in agreement with this interpretation. Therefore, the true values of the reaction probability will be some 10% above the $p_1 = 0.083$ data points, which are about 0.3 for both 1010 and 300 K.

The reaction probability values for the oxidation reaction (1), taken from Ref. 5, are shown for comparison. As Fig. 12 shows, the nitridation coefficient is substantially larger than the oxidation coefficient.

As mentioned in the "Introduction" section, the nitridation process under study is equivalent to the surface catalytic recombination process in a typical boundary-layer flow. The reaction coefficient of

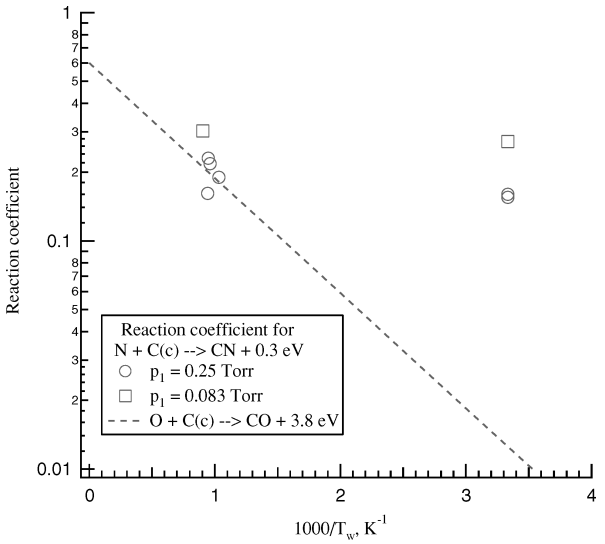


**Fig. 12 Arrhenius plot of reaction probability of nitridation of solid carbon.**

nitridation becomes an effective recombination coefficient in this case. The coefficient value of 0.3 is nearly that of clean metals with high catalytic coefficients such as copper.[14] Thus, for the boundary-layer flow, the ablating carbonaceous material is likely to behave as a highly catalytic wall for nitrogen recombination.

## Future Work

The present work relies partly on the accuracy of the radiation model assumed. It is desirable that the detailed spectrum of the flow in the concerned wavelength region, from about 370 to about 410 nm, be obtained to confirm the accuracy of the radiation model. At the time of the work reported herein, the spectrograph needed for that purpose was out of commission. The work could be repeated with the needed instrument to obtain a detailed spectrum.

The largest uncertainty in the present work concerns the fact that the intensity of the CN radiation increases with time for the case of $p_1 = 0.25$ torr (Fig. 9) as mentioned earlier, which may be due to the outgassing of the carbon coating. A more complete graphitization of the carbon should be carried out to remove the doubt about outgassing of the coating. Graphitization could be improved by changing to a vacuum vapor deposition technique instead of the lampblack technique. Vapor deposition of carbon could be carried out by exposing the tungsten wire grid to a glow discharge in methane.

The reaction probability is determined assuming a free-molecular flow. For the case of $p_1 = 0.25$ torr, the Knudsen number is typically unity. For this case, a correction may be necessary to account for the collisions among the gas molecules. Also, tests could be made at other $p_1$ values to ascertain a systematic trend of the effect of varying Knudsen number.

Last, more tests should be made to increase the total number of data points to improve the statistical accuracy of the measurements.

## Conclusions

The coefficient of reaction of nitrogen atoms with solid carbon was determined by comparing the numer density of CN molecules, determined from the measured intensity of CN radiation, with the calculated number density of N atoms in the wake of a grid of metal wires coated with solid carbon placed in a shock-tube flow. The experiment shows an unexplained temporal variation in the concentration of CN. This phenomenon must be understood or eliminated for the test results to be interpreted unambiguously. However, based on the CN concentration values before the onset of this temporal variation, the coefficient of reaction of nitrogen atoms with graphitic solid carbon is deduced to be approximately 0.3 at both 300 and 1100 K, with a scatteer of a factor of 1.5. More measurement could be made to remove the uncertainty and to improve the statistical accuracy of the measurements.

## Acknowledgments

The authors wish to acknowledge the support provided by the Director's Discretionary Fund of NASA Ames Research Center and by Contract NAS2-99092 to Eloret Corporation. They wish also to thank Richard Exberger of NASA Ames Research Center for the various innovations introduced in the design of the apparatus and in their operation.

## References

[1]Olynick, D. R., Chen, Y. K., and Tauber, M. E., "Forebody TPS Sizing with Radiation and Ablation for the Stardust Sample Return Capsule," AIAA Paper 97-2474, June 1997.

[2]Yamada, T., Hiraki, K., Ishii, N., and Inatani, Y., "Thermal Protection System of MUSES-C Reentry Capsule," *Proceedings of the 21st International Symposium on Space Technology and Science*, Vol. 1, Sonic City, Oyama, Japan, May 1998, pp. 782–787.

[3]Park, C., "Interaction of Spalled Particles with Shock Layer Flow," *Journal of Thermophysics and Heat Transfer*, Vol. 13, No. 4, 1999, pp. 441–449.

[4]Park, C., Raiche, G. A., II., and Driver, D. M., "Radiation of Spalled Particles in Shock Layers," *Journal of Thermophysics and Heat Transfer*, Vol. 18, No. 4, 2004, pp. 519–526.

[5]Park, C., "Effects of Atomic Oxygen in Graphite Ablation," *AIAA Journal*, Vol. 14, No. 11, 1976, pp. 1640–1642.

[6]Chen, Y. K., and Milos, F. S., "Finite-Rate Ablation Boundary Conditions for a Carbon–Phenolic Heat-Shield," AIAA Paper 2004-2270, June 2007.

[7]Sepka, S., Chen, Y. K., and Marshall, J., "Experimental Investigation of Surface Reactions in Carbon Monoxide and Oxygen Mixtures," *Journal of Thermophysics and Heat Transfer*, Vol. 14, No. 1, 2000, pp. 45–52.

[8]Sharma, S. P., and Park, C., "Operating Characteristics of 60- and 10-cm Electric Arc-Driven Shock Tubes, Part 1: The Driver," *Journal of Thermophysics and Heat Transfer*, Vol. 4, No. 3, 1990, pp. 259–265.

[9]Sharma, S. P., and Park, C., "Operating Characteristics of 60- and 10-cm Electric Arc-Driven Shock Tubes, Part 2: The Driven Section," *Journal of Thermophysics and Heat Transfer*, Vol. 4, No. 3, 1990, pp. 266–272.

[10]Whiting, E. E., Park, C., Liu, Y., Arnold, J. O., and Paterson, J. A., "NEQAIR96, Nonequilibrium and Equilibrium Radiative Transport and Spectra Program: User's Manual," NASA Reference Publ. 1389, Dec. 1996.

[11]Park, C., "On Convergence of Computation of Chemically Reacting Flows," *Thermophysical Aspects of Re-Entry Flows*, Vol. 103, edited by J. N. Moss and C. D. Scott, Progress in Astronautics and Aeronautics, AIAA, New York, 1986, pp. 478–513.

[12]Sharma, S. P., and Gillespie, W., "Nonequilibrium and Equilibrium Shock Front Radiation Measurements," *Journal of Thermophysics and Heat Transfer*, Vol. 5, No. 3, 1991, pp. 257–265.

[13]Dean, A. J., Hanson, R. K., and Bowman, C. T., "High Temperature Shock Tube Study of Reactions of CH and C-Atoms with $N_2$," *23rd Symposium (International) on Combustion*, Combustion Inst., Pittsburgh, PA, 1990, pp. 259–265.

[14]Goulard, R., "On Catalytic Recombination Rates in Hypersonic Stagnation Heat Transfer," *Jet Propulsion*, Vol. 28, No. 11, 1958, pp. 737–745.